Simple models of human brain functional networks

Petra E. Vértes[a], Aaron F. Alexander-Bloch[a,b,c], Nitin Gogtay[b], Jay N. Giedd[b], Judith L. Rapoport[b], and Edward T. Bullmore[a,d,e,1]

[a]Department of Psychiatry, Behavioural and Clinical Neuroscience Institute, University of Cambridge, Cambridge CB2 0SZ, United Kingdom; [b]Child Psychiatry Branch, National Institute of Mental Health, Bethesda, MD 20892-1600; [c]David Geffen School of Medicine at University of California, Los Angeles, CA 90095; [d]Cambridgeshire and Peterborough National Health Service Foundation Trust, Cambridge CB21 5EF, United Kingdom; and [e]GlaxoSmithKline Clinical Unit Cambridge, Addenbrookes Hospital, Cambridge CB2 0QQ, United Kingdom

Edited by Michael S. Gazzaniga, University of California, Santa Barbara, CA, and approved February 21, 2012 (received for review August 1, 2011)

Human brain functional networks are embedded in anatomical space and have topological properties—small-worldness, modularity, fat-tailed degree distributions—that are comparable to many other complex networks. Although a sophisticated set of measures is available to describe the topology of brain networks, the selection pressures that drive their formation remain largely unknown. Here we consider generative models for the probability of a functional connection (an edge) between two cortical regions (nodes) separated by some Euclidean distance in anatomical space. In particular, we propose a model in which the embedded topology of brain networks emerges from two competing factors: a distance penalty based on the cost of maintaining long-range connections; and a topological term that favors links between regions sharing similar input. We show that, together, these two biologically plausible factors are sufficient to capture an impressive range of topological properties of functional brain networks. Model parameters estimated in one set of functional MRI (fMRI) data on normal volunteers provided a good fit to networks estimated in a second independent sample of fMRI data. Furthermore, slightly detuned model parameters also generated a reasonable simulation of the abnormal properties of brain functional networks in people with schizophrenia. We therefore anticipate that many aspects of brain network organization, in health and disease, may be parsimoniously explained by an economical clustering rule for the probability of functional connectivity between different brain areas.

neuroimaging | graph theory | systems | trade-off

The human brain is a large and complex network, operating over several decades of scale in space and time (1, 2). Its organization defies complete description at a cellular scale (3); but neuroimaging techniques for whole-brain scanning have been used to describe network organization, or connectomics, at anatomical scales on the order of millimeters and centimeters (2). In the language of graph theory, these large-scale human brain networks have already been shown consistently to demonstrate a number of key topological properties in common with other complex networks. For example, human brain networks have the small-world property of high clustering and high efficiency (or short path length) (4); they are also modular (5) and comprise a number of highly connected hub nodes in a fat-tailed degree distribution (6).

It is well known that the brain overall is expensive, in the sense of having high metabolic cost relative to its mass (7), and that cost control or cost minimization is likely to have been an important selection criterion for the evolution of the nervous system (8–11). One measure of cost in a spatially embedded network like the brain is the physical distance of connections between nodes: generally, connection costs will increase with distance (8, 12). In the nervous system of the nematode worm *Caenorhabditis elegans*, which has been mapped completely at the cellular level of synaptic connections between neurons (13), most axonal projections are shorter than the average distance between neurons, as expected in response to an economical selection pressure (14, 15). Likewise, in sparsely connected human brain functional networks, short distance connections predominate and are typically associated with greater strength of functional connectivity between regional nodes (16).

Given these observations on the topologically complex and anatomically economical aspects of brain networks, we asked this question: what set of generative factors could explain the topology of anatomically embedded brain networks? To address this question, we consider simple models for the probability of functional connection (an edge) between two cortical areas (nodes) separated by some Euclidean distance in anatomical space (≈cm). The simplest (one-parameter) models specify that connection probability is a function only of distance between nodes (17, 18), but we show that cost penalization alone cannot account for the small-worldness, modularity, and degree distribution of normal human brain functional networks. Two-parameter models specify that connectivity is a function of distance and the topological properties of the connected nodes (19). We show that a two-parameter model, for example including a "clustering" function of nodal topology as well as a power law function of connection distance, is required to emulate many of the key topological and anatomical statistics of normal brain functional networks.

We used resting-state functional MRI (fMRI) to measure low-frequency neurophysiological oscillations at each of 140 cortical brain regions in the right hemisphere in two groups of 20 healthy volunteers and 19 participants with childhood-onset schizophrenia (COS). We estimated functional connectivity by the correlation between each pair of regional time series; and we thresholded the resulting connectivity matrices to generate sparse, fully connected graphs (*Materials and Methods*).

Results

For each graph, we measured global efficiency [a measure of network integration inversely related to path length (20)]; average clustering coefficient (a measure of cliquish interconnections between topologically neighboring nodes); modularity [a measure of how nearly the network can be decomposed into a set of sparsely interconnected modules, each comprising several densely intraconnected nodes (21)]; the degree distribution (the probability distribution of degree, or number of edges per node); and the distance distribution (the probability distribution of Euclidean distance between connected pairs of regions) (Fig. 1). These data confirmed prior reports of economical small-worldness, modularity, and hub nodes in human brain networks (2).

Exponential Decay with Distance. To investigate the extent to which the topological profile of the brain networks could be attribut-

Author contributions: P.E.V., A.F.A.-B., and E.T.B. designed research; P.E.V. performed research; N.G., J.N.G., and J.L.R. contributed new reagents/analytic tools; P.E.V. and A.F.A.-B. analyzed data; and P.E.V. and E.T.B. wrote the paper.

The authors declare no conflict of interest.

This article is a PNAS Direct Submission.

Data deposition: The raw time series, correlations, and binary graphs reported in this paper for the primary group of healthy volunteers are available from the National Institute of Mental Health, http://intramural.nimh.nih.gov/chp/articles/matlab.html. The link also provides access to the binary graphs constructed for the group with COS.

[1]To whom correspondence should be addressed. E-mail: etb23@cam.ac.uk.

This article contains supporting information online at www.pnas.org/lookup/suppl/doi:10.1073/pnas.1111738109/-/DCSupplemental.

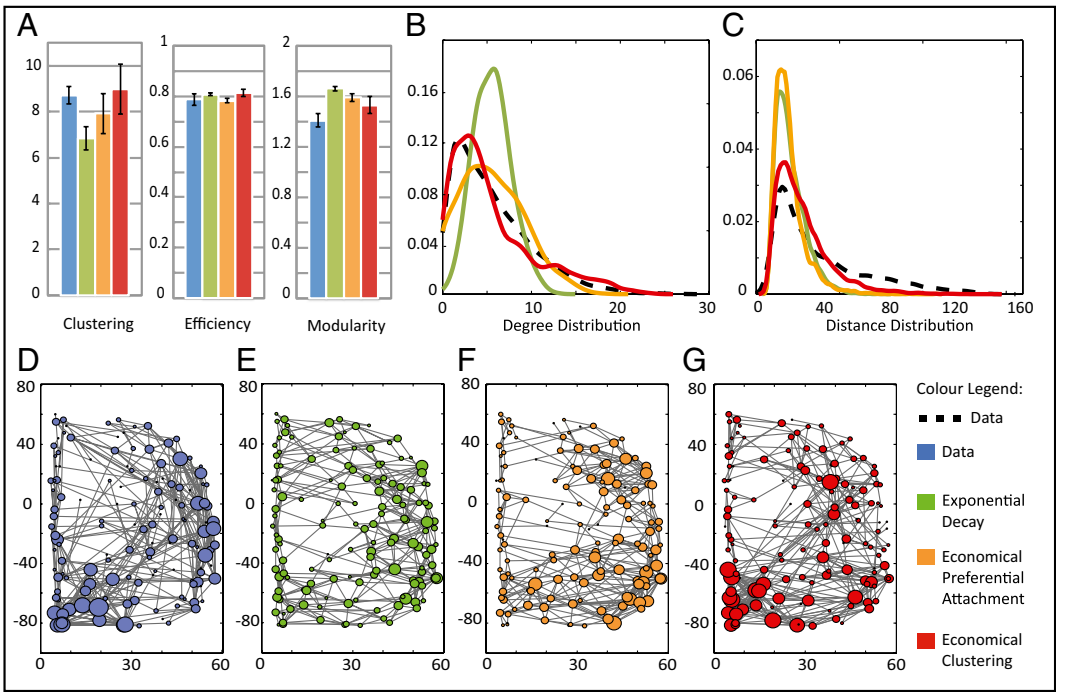

Fig. 1. Comparison of networks simulated by three generative models vs. brain functional networks derived from experimental fMRI data on a group of 20 healthy volunteers (blue). Both the simple one-parameter model based on an exponential distance penalty (green) and the two-parameter economical preferential attachment model (orange) fail to simultaneously capture several topological characteristics of functional brain networks. In contrast, the economical clustering model (red) yields significantly more realistic networks by all of the following measures. (*A*) Normalized clustering coefficient, global efficiency, and modularity of brain functional networks are all well matched by the economical clustering model. All values are averaged over 20 instantiations of each network, and error bars represent the 95% confidence interval for the mean. Degree (*B*) and distance (*C*) distributions are shown in solid colored and dashed black lines for the models and data, respectively. Both distributions are better captured by the economical clustering model (red) than by the exponential decay (green) or economical preferential attachment (orange) models. (*D*–*G*) Schematic representation of the right hemisphere of the fMRI brain network for one participant (blue) and of a representative network generated by a single instantiation of each model. To ensure that these networks are representative, the single participant and the specific model instantiations displayed were each chosen to have the median value of skew in their degree distributions. The size of each node represents the degree of the corresponding brain region within the network. All networks have an overall connection density of 4% and comprise 140 nodes.

able solely to cost minimization, we adopted a simple model for the probability of connection $P_{i,j}$ between any pair of regions as a function of the distance between them (17, 18):

$$P_{i,j} \propto \exp(-\eta d_{i,j}), \qquad [1]$$

where $d_{i,j}$ is the anatomical distance between regions i and j, and η is the only parameter of the model. Using this exponential decay model with a range of different values of η, we could generate networks with variable degrees of cost penalization dictating the probability of connection between nodes.

We found, for example, that at a certain value of the model parameter, $\eta \approx 0.09$, the simulated networks had an average modularity that matched exactly the modularity of the brain networks. However, these simulated data failed to match the empirical networks well in terms of global efficiency, clustering, or degree distribution. Indeed, it can be shown that there is no single value of η that will generate networks that are well matched to brain networks in terms of both modularity and efficiency (*SI Text 1*, Fig. S1). When η is large and distance penalization is high, the networks are not as efficient as brain networks, owing to the lack of long-distance connections; whereas when η is small the modeled networks are not as modular as the empirical ones. To find the compromise value of η that overall best fits the data, we used simulated annealing (SA) on an energy function based on the P values for the difference in clustering, efficiency, modularity, and degree distribution between a set of model networks and the data (*Materials and Methods* and *SI Text 2, 3, and 4*). As expected, however, the model-generated networks were not able to match simultaneously all key network characteristics observed in the data (Fig. 1). Similar results were obtained using other models of decay in connection probability as a function of distance [e.g., the power law model $P_{i,j} \propto (d_{i,j})^{-\eta}$]. In general, it seems that penalizing connection probability by a function of distance alone will be insufficient to simulate the topological statistics of brain functional networks (Table S1).

Economical Preferential Attachment. Growth models for the formation of other real-life complex systems have previously been more successful by including an additional topological term in the connection probability function (19, 22), for example:

$$P_{i,j} \propto (k_i k_j)^{\gamma} (d_{i,j})^{-\eta}. \qquad [2]$$

Here, $P_{i,j}$ is the probability of connecting nodes i and j, of degree k_i and k_j, respectively, that are a distance $d_{i,j}$ apart; η is the parameter of distance penalization, as before; γ is the parameter of preferential attachment (the exponent of a power law in the product of the degrees of the connected nodes). Intuitively, this model trades off the cost-minimizing drive to shorter connection distance against the tendency to form highly connected hubs. The best-fitting parameters (estimated by SA) generated better approximations of brain networks than those simulated by cost penalization alone: the degree distribution was more realistically fat-tailed; and global efficiency, clustering, and modularity were all closer to their experimental benchmarks (Fig. 1 and Table S1).

These results support the general principle that cost minimization is likely to be a necessary but not a sufficient criterion for

formation of brain networks. To more fully account for the observed characteristics of brain networks, we need to assume some complementary or countervailing generative factors that promote the emergence of complex topological features, such as the existence of hubs.

Economical Clustering Model. We explored other possible variants of Eq. **2**, using various functions of the degrees of the connected nodes to weight the formation of complex topological features, and tested each model against the same set of experimental benchmark data on human fMRI networks (Table S1). The best-fitting of these connection probability models included a power law distance penalty, as before, as well as a power law function of a topological term,

$$P_{i,j} \propto (k_{i,j})^{\gamma}(d_{i,j})^{-\eta}, \qquad [3]$$

where $k_{i,j}$ is the number of nearest neighbors in common between nodes i and j; and all other notation is identical to Eq. **2**. We will refer to this as an "economical clustering" model that includes a negative bias against high connection cost and a positive bias in favor of consolidating connectivity between nodes having nearest neighbors in common.

Optimizing the parameters of this economical clustering model to match the topological profile of brain networks, we found good correspondence ($P > 0.05$) between the simulated and fMRI networks on all of the key topological metrics of global efficiency, clustering, and modularity. Overall, the simulated networks were significantly more brain-like than either of the models previously considered (Fig. 1 and Table S1). We found these results to hold for brain networks thresholded over a range of connection densities, from 4% to 16% of all possible edges between regional nodes (*SI Text 5* and Table S2). An intuitive understanding of the role of each parameter in this model can be gained by plotting a phase diagram (Fig. 2) highlighting the regions in parameter space that lead to small-world and heavy-tailed (skew $S > 1$) networks. We also plot schematics of the networks obtained by varying each parameter separately, from zero to their experimentally estimated values ($\eta = 2.63$, $\gamma = 3.17$). These two sections through parameter space confirm that variations in η mainly affect the distance distribution, whereas tuning γ mainly influences the degree distribution (Figs. S2 and S3).

However, because the model parameter estimation (by SA; *SI Text 2* and Fig. S4) has minimized the mismatch between an observed dataset and simulated values of network metrics (*SI Text 3* and Figs. S5–S7), one might argue that it is not so surprising that the fitted model is able to reproduce these same properties quite accurately. To address this potential issue of circularity, we did two things.

First, we explored the model's capacity to simulate brain network properties that had not been directly used as a basis for parameter estimation. For example, as shown in Fig. 1, we found that the distance distribution in the experimental fMRI networks was reasonably well matched by the economical clustering model (in comparison with the other models considered). We also found that annealing without any constraints on the degree distribution resulted in model parameters very similar to those estimated by annealing over all four network topological properties, with correspondingly good fits to all fMRI network metrics, including the degree distribution (*SI Text 6.1* and Fig. S8). Additionally, as shown in Fig. 3, we found that the economical clustering model (in contrast to Eq. **1** and Eq. **2**) also captured the statistical distribution of topological measures—such as the clustering and efficiency—at the local level of individual nodes in the fMRI networks, although the annealing process had been constrained

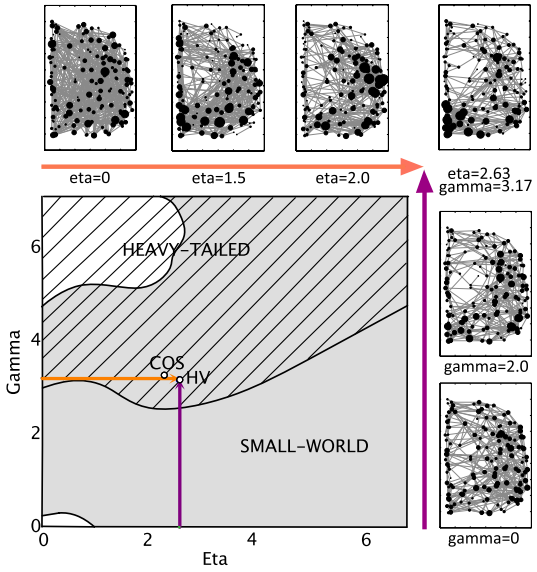

Fig. 2. Phase diagram of the economical clustering model. Most values of eta (η) and gamma (γ) yield small-world networks (gray area), whereas only high values of γ yield networks with heavy-tailed (skew >1) degree distribution (hashed area). The model parameters estimated to minimize mismatch between simulated and experimental fMRI datasets are shown here for both healthy volunteers (HV) and participants with childhood onset schizophrenia (COS). The orange (and purple) arrows show sections through the phase space, varying only η (or γ) respectively, whereas the other parameter is held at its optimal value estimated in healthy volunteers. Schematics of the networks obtained at various points along these sections are also shown (along zoomed-in versions of the orange and purple arrows).

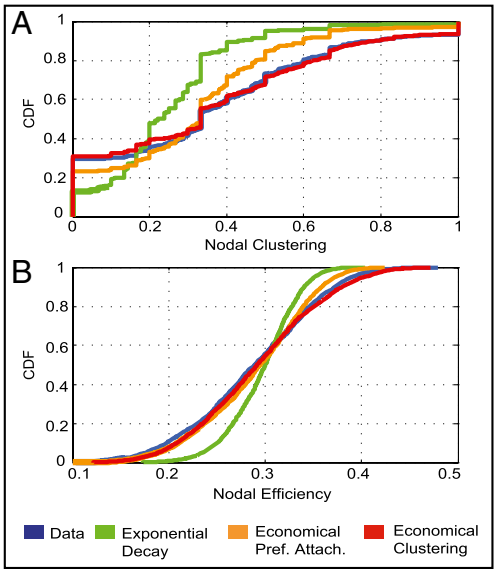

Fig. 3. Simulation of network parameters not involved in model parameter estimation. The exponential decay model (expD), economical preferential attachment model (ecoPA), and economical clustering model (ecoC) are shown in green, orange, and red, respectively. Of these, only the economical clustering model generates networks that realistically approximate the experimental (fMRI; blue) distributions of nodal topological metrics, such as clustering (*A*) and efficiency (*B*), that were not included in the process of model parameter estimation. The *P* values from a Kolmogorov-Smirnov test comparing the cumulative distributions for each parameter between the modeled and experimental networks are: $P_{expD} = 10^{-103}$, $P_{ecoPA} = 10^{-20}$, and $P_{ecoC} = 0.04$ for nodal clustering; and $P_{expD} = 10^{-45}$, $P_{ecoPA} = 6{\cdot}10^{-4}$, and $P_{ecoC} = 0.035$ for nodal efficiency.

only by the global average of these measures over all nodes in the networks.

Second, we used the generative model parameters estimated from the primary fMRI dataset (n = 20 healthy volunteers) to predict the network properties of a second independent fMRI dataset (n = 12 healthy volunteers). Thus, we tested the goodness of fit of the model on a set of experimental data that had not been used for model estimation. The economical clustering model provided a good account (compared with Eq. **1** and Eq. **2**) of the statistical distributions of efficiency, clustering, modularity, degree, and connection distance in this independent test dataset (*SI Text 6.2* and Fig. S9).

Modeling Network Changes in Schizophrenia. We measured fMRI network properties experimentally in 19 people with COS and estimated economical clustering model parameters from these clinical data. Consistent with prior studies of functional connectivity and functional network organization in schizophrenia, we found that topological properties of clustering and modularity were somewhat reduced in COS patients (23–26). The abnormal profile of brain network topology in the patient group could be reasonably well matched by the economical clustering model (*SI Text 7* and Fig. S10) but with rather different model parameters ($\eta = 2.3, \gamma = 3.33$) compared with those estimated in the group of healthy volunteers ($\eta = 2.63$, $\gamma = 3.17$). This shift in optimal parameter settings shows that the abnormal organization of brain functional networks in schizophrenia can be modeled as the outcome of an abnormally biased tradeoff between the generative factors of distance penalization and topological clustering.

Discussion

We have explored a number of generative models to parsimoniously simulate the complex topological and anatomical properties of human brain functional networks. We have shown that the simplest models considered, which penalize the probability of a functional connection between brain network regions as a function of the anatomical distance between them, cannot satisfactorily account for the complex topological properties of real brain networks. This result argues against the position that brain organization can be explained entirely by the principle of cost minimization (Table S4). However, we found that the addition of a topological term to the model, favoring additional formation of connections between nodes that already share nearest neighbors in common, could markedly improve the simulation of realistic brain network properties. This economical clustering model provided a good account of several network properties that were not included in the process of model parameter estimation, and when estimated in one normal sample, provided a good fit to the network properties of a second, independent normal sample.

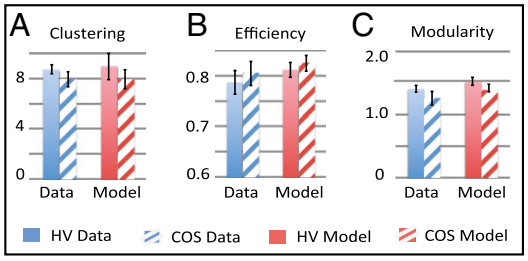

Fig. 4. The economical clustering model is adaptive to fMRI network abnormalities in children with childhood onset schizophrenia (COS). COS (hashed bars) is associated with shifts in clustering, efficiency, and modularity (*A*–*C*) of fMRI networks, compared with the same metrics in fMRI networks of healthy volunteers (HV; solid bars). The bar charts on the right-hand side of each panel show the corresponding metrics simulated by the economical clustering model for both groups. See also *SI Text 7* and Table S3.

Prior models for formation of brain anatomical networks have emphasized the importance of controlling or penalizing connection distance (17, 18). This is consistent with a large body of work, dating back to the seminal studies of Ramón y Cajal in the 19th century, indicating that the material and metabolic costs of the brain are large in proportion to its mass and that cost control is an important principle of brain organization (14). Because the metabolic cost of a connection between brain regions increases with increasing anatomical distance, cost minimization would be expected to drive the formation of connections between anatomically neighboring nodes. There are aspects of adult brain organization that are consistent with this expectation. For example, the probability distribution of connection distances in human brain networks is skewed toward shorter distances (27). The modules of brain networks also typically comprise brain regions that are anatomical as well as topological neighbors (28); so intramodular connections, which predominate in highly modular brain networks, are generally short distance.

However, it is also clear that brain networks have a high global efficiency (or short characteristic path length) that is largely attributable to the existence of long distance connections between anatomically localized modules (27). The efficiency of brain networks is a measure of their capacity for integrated processing, and several studies have shown that greater efficiency of network topology is associated with higher intelligence quotient (29, 30), greater accuracy of working memory task performance (31), or successful performance of more difficult versions of a working memory task (32). Thus, the topological attribute of high efficiency seems empirically to be important for cognitive functions of human brain networks, as also anticipated hypothetically by global workspace theory (33, 34). This is clearly difficult to reconcile with the unchallenged primacy of a cost conservation principle. Indeed, it has been shown by computational "rewiring" of the anatomical networks of *C. elegans* and the macaque monkey cortex that total connection distance of both these networks is not strictly minimized in nature; and when it is strictly minimized *in silico* there is a complementary increase in path length (or decrease in global efficiency) of the minimally rewired networks (35).

The idea that emerges from these and other prior studies is that brain network formation cannot plausibly be modeled by cost minimization alone but must rather depend on some "tradeoff," between distance penalization and one or more other factors, which allows the emergence of realistically complex network topology (10, 36, 37). The results presented here provide some specific examples of how such a tradeoff might be rigorously defined and the considerable improvements in accuracy of brain network modeling that ensue as a result.

We investigated several possible models of competition or tradeoff between a distance penalization term and a second term weighting formation of particular topological features. The first model (Eq. **2**) has been previously used to simulate the organization of the Internet (19). This economical preferential attachment model increases the probability of a connection between nodes in proportion to their degrees. Thus, high-degree nodes or hubs are more likely to form additional connections, even if separated by considerable distances. Although addition of a preferential attachment term improved the capacity of the model to capture a range of brain network properties (compared with the simpler models of distance penalization), we found empirically that alternative two-parameter models simulated experimental data even more accurately. In total, we evaluated 12 possible generative models (Table S1), varying both the cost penalization and topological terms, and found that the most accurate model overall (Eq. **3**) traded-off connection distance against a topological term favoring the formation of connections between nodes that already shared nearest neighbors. Besides these empirical results indicating superior goodness of fit for one model in comparison with others, how else can we justify a preference for this economical clustering model?

First, we note that both terms of the model have some degree of face validity as biological mechanisms for brain network formation. Distance penalization, as has previously been noted (17), could be mediated mechanistically by the distance-related fall-off in concentration gradients of growth factors directing axonal projections toward target neurons. Enhanced probability of connection between neurons that already share nearest neighbors was recently observed in the rat somatosensory cortex (38). This is also compatible with Hebb's law, in the sense that neuronal groups that share common inputs from the same topologically neighboring group are more likely to be simultaneously activated and therefore to consolidate direct connections. We note that such biologically mechanistic interpretations of model parameters are no more than heuristics, and require more rigorous testing experimentally; nevertheless it is conceptually easier to imagine how local clustering might be favored (by Hebbian mechanisms) than to imagine how a preferential attachment rule might operate biologically. Indeed, unlike in engineered systems, it is unclear how any component of a brain network would have information on the degrees of all of the other nodes in the system.

Second, we note that the economical clustering model, as well as providing the most accurate simulation of global and nodal network parameters in fMRI data acquired from healthy volunteers, was also adaptive to the rather different network properties of data from people with COS. Previous studies have quite consistently demonstrated a topological profile of "subtle randomization" in schizophrenia (39), which was confirmed in these data by somewhat reduced clustering and modularity and increased global efficiency. This topological shift toward a more random configuration was simulated by a generative model with an abnormally reduced distance penalization parameter, allowing a greater probability of long distance connections. This result echoes some prior neuroimaging results, suggesting that brain networks in schizophrenia may have a greater than normal proportion of long-distance connections (27, 40) and encourages future efforts to use the modeled parameters of network formation to summarize and understand the patterns of abnormal network topology seen in people with a neurodevelopmental disorder such as schizophrenia (41, 42), as well as the processes of topological and spatial reconfiguration of human brain networks that may occur in the course of normal maturation to adulthood (43, 44).

This study also raises a number of methodological and conceptual questions (further discussion is provided in *SI Text 2–4 and 8*). The brain networks were constructed from fMRI time series, which have good anatomical resolution but insufficiently refined time resolution to allow estimation of high frequency dynamics or conduction delays, although these are likely to be important parameters of brain network performance. Moreover, the functional connectivity between a pair of nodes (e.g., as measured by the correlation between time series) cannot be assumed certainly to indicate that there is direct anatomical connectivity between them (45). Thus, there are empirical limits on what we can infer from these data about the mechanistic or domain-specific details of human brain network function and structure. In this context, we have adopted a modeling strategy that has been widely explored in the context of other complex networks, but not before so thoroughly developed in a neuroscientific application. We formulated some relatively simple generative models and tested their capacity to emulate the topological properties observed in brain networks. The existence of a good fit for some of these models, although statistically robust, does not prove that the brain networks were naturally selected to optimize the model parameters. The function(s) (if any) optimized by natural selection of brain networks are not yet known. So modeling brain networks cannot certainly begin from an optimality function, as one might begin to analyze or design an artificial network for which the desired function was known (46). However, a stochastic approach to brain network modeling is both tractable and arguably reasonable, given the stochastic contribution to selection of brain networks in real life. Our results show that brain network statistics can be generated quite accurately by simple (but not the simplest) probabilistic models.

Conclusion

Human brain functional networks have a complex topology, embedded in anatomical space, which can be modeled as the outcome of a tradeoff between two factors: a constraint on connection distance and a tendency for clustered connections. This is consistent with the general principle that cost minimization alone is insufficient to explain brain network organization and suggests that diverse brain network phenomena, in health and disease, may be explicable in terms of tradeoffs between a small number of biologically plausible generative factors.

Materials and Methods

Sample, Image Acquisition, and Analysis. The fMRI data were acquired from two groups of healthy volunteers: a primary group (evaluable data on $n = 20$; mean age 19.7 y; 11 male) and a secondary group ($n = 12$; mean age 17.5 y; 6 male). The primary group of 20 healthy volunteers matched 19 participants meeting the DSM-IV criteria for COS (mean age 18.7; 9 male), recruited as part of an National Institutes of Health (NIH) study of COS and normal brain development. This study was ethically approved by the local institutional review board, and consent was acquired from all participants as well as their legal guardians. Excessive head motion during fMRI was an exclusion criterion. There were no significant differences between the groups in terms of age, sex, or maximum displacement due to head motion (details in *SI Text*). Participants were scanned using a General Electric Signa MRI scanner operating at 1.5 T, at the NIH Clinical Center in Bethesda, MD. One anatomical T1-weighted fast spoiled gradient echo MRI volume was acquired: echo time (TE) 5 ms; relaxation time (TR) 24 ms; flip angle 45°; matrix 256 × 256 × 124; field of view (FOV) 24 cm. Two sequential 3-min echo-planar imaging (EPI) scans were acquired while the participants were lying quietly in the scanner with eyes closed: TR 2.3 s; TE 40 ms; voxel 3.75 × 3.75 × 5 mm; matrix size 64 × 64; FOV 240 × 240 mm; 27 interleaved slices.

The images were preprocessed on the high-performance NIH Biowulf Linux cluster (http://biowulf.nih.gov), using AFNI (47) and FSL (48, 49) software. The first four EPI images were discarded to account for T1 equilibration effects. The data were then despiked, motion-corrected, skull-stripped, and registered to each participant's structural scan. Structural scans were registered to the standard stereotactic space of the Montreal Neurological Institute (MNI), using the MNI adult brain template (50, 51). Cerebrospinal fluid (CSF) and white matter were segmented with a probability threshold of 0.8. The time series for each voxel was regressed against the average CSF and white matter signals as well as the six parameters from motion correction, with all further analysis based on the residuals. Gray matter areas were defined using FSL's cortical Harvard-Oxford probabilistic atlas thresholded at 25%, excluding voxels that did not provide fMRI coverage in every participant. Voxels were then downsampled to ≈300 approximately uniform regions (52), maximizing compactness, and under the constraints that no brain regions spanned hemispheres or cortical lobes or extended over more than twice the size of the smallest region. We focused on regions in the right hemisphere to facilitate the approximation of the wiring length by the Euclidean distance between brain regions (44). This resulted in 140 regions whose average time series were used to construct brain functional networks. The maximal overlap discrete wavelet transform with a Daubechies 4 wavelet was used to band-pass filter these time series to the frequency interval: 0.05–0.111 Hz (scale 2). These preprocessed data can be downloaded for the primary group of healthy volunteers via http://intramural.nimh.nih.gov/chp/articles/matlab.html. The link also provides access to the graphs constructed for both the primary healthy volunteer and COS groups.

Graph Construction. Binary graphs were constructed by thresholding the wavelet correlation matrix estimated for each participant. To ensure that no nodes were disconnected from the rest of the network, we used the minimum spanning tree as a backbone, then added further edges in order of decreasing correlation strength to produce binary graphs over a range of connection densities (26), from 4% to 16% of the maximum possible number of connections between N nodes. Networks simulated by generative models were likewise fully connected and controlled for connection density. All topological measures were normalized by dividing by the equivalent measures estimated from random graphs with the same number of nodes and edges.

Network Measures. The graphs thus constructed were topologically analyzed using some of the most widely used graph theoretical network metrics (efficiency,

clustering modularity, and degree); we note that these metrics are also directly related or very similar to some other well-known graph metrics (such as local efficiency, path length, or the small-world ratio of clustering to path length).

The degree, k_i, of a node i represents the number of edges connecting it to the rest of the network. The degrees of all of the nodes of a graph G form the degree distribution. The clustering coefficient C_i is defined as the ratio of the number of triangular connections between the ith node's nearest neighbors to the maximal possible number of such triangular motifs. The overall clustering coefficient $C(G)$ is defined as the average clustering coefficient of all nodes. The path length $L_{i,j}$ between a pair of nodes i and j is defined as the minimum number of edges that need to be traversed to get from i to j. More commonly (20), one measures the average inverse path length, or global efficiency, $0 < E(G) < 1$. Many complex networks have a modular community structure, whereby they contain subsets of highly interconnected nodes called modules. The modularity, $Q(G)$, of a graph quantifies the quality of a suggested partition of the network into modules by measuring the fraction of the network's edges that fall inside modules compared with the expected value of this fraction if edges were distributed at random (21). The maximum value, $M(G)$, of the modularity found for any partition of a given graph into modules yields a measure of the degree of modularity of the network, compared with random networks.

Model Parameter Estimation. The optimal parameters η and γ used for each model were estimated by SA on an energy function defined as

$$E = \frac{1}{P_C.P_E.P_M.P_k}$$

where P_C is the P value associated with the t test for a difference in the mean clustering coefficients of a set of 20 simulated model networks vs. a set of 20 experimental fMRI datasets (more details are provided in *SI Text 2–4*). Similarly, P_E and P_M are P values of t tests for the difference between efficiency and modularity in modeled vs. experimental data, whereas P_k is the P value of the Kolmogorov-Smirnoff test between the degree distributions estimated from the simulated and experimental networks. SA aims to find the minimum of the energy function in parameter space, and thus finds the η and γ parameters that generate model networks that most closely approximate the experimental data in terms of clustering, efficiency, modularity, and degree distribution.

ACKNOWLEDGMENTS. The Behavioural and Clinical Neuroscience Institute is supported by the Wellcome Trust and the Medical Research Council. P.E.V. was supported by a grant from the Engineering and Physical Sciences Research Council. Data collection was supported by the intramural research program of the National Institute of Mental Health, NIH. A.F.A.-B. is supported by the NIH Cambridge Graduate Partnership Program.

1. Stam CJ, Reijneveld JC (2007) Graph theoretical analysis of complex networks in the brain. *Nonlinear Biomed Phys* 1:3.
2. Bullmore E, Sporns O (2009) Complex brain networks: Graph theoretical analysis of structural and functional systems. *Nat Rev Neurosci* 10:186–198.
3. Sporns O, Tononi G, Kötter R (2005) The human connectome: A structural description of the human brain. *PLOS Comput Biol* 1:e42.
4. Watts DJ, Strogatz SH (1998) Collective dynamics of 'small-world' networks. *Nature* 393:440–442.
5. Meunier D, Lambiotte R, Bullmore ET (2010) Modular and hierarchically modular organization of brain networks. *Front Neurosci* 4:200.
6. Achard S, Salvador R, Whitcher B, Suckling J, Bullmore E (2006) A resilient, low-frequency, small-world human brain functional network with highly connected association cortical hubs. *J Neurosci* 26:63–72.
7. Laughlin SB, Sejnowski TJ (2003) Communication in neuronal networks. *Science* 301: 187–1874.
8. Cherniak C (1994) Component placement optimization in the brain. *J Neurosci* 14: 2418–2427.
9. Klyachko VA, Stevens CF (2003) Connectivity optimization and the positioning of cortical areas. *Proc Natl Acad Sci USA* 100:7937–7941.
10. Chklovskii DB, Schikorski T, Stevens CF (2002) Wiring optimization in cortical circuits. *Neuron* 34:341–347.
11. Cherniak C, Mokhtarzada Z, Rodriguez-Esteban R, Changizi K (2004) Global optimization of cerebral cortex layout. *Proc Natl Acad Sci USA* 101:1081–1086.
12. Barthélemy M (2011) Spatial networks. *Phys Rep* 499:1–101.
13. White JG, Southgate E, Thomson JN, Brenner S (1986) The structure of the nervous system of the nematode *C. elegans*. *Philos Trans R Soc Lond B Biol Sci* 314:1–340.
14. Niven JE, Laughlin SB (2008) Energy limitation as a selective pressure on the evolution of sensory systems. *J Exp Biol* 211:1792–1804.
15. Chklovskii DB (2004) Exact solution for the optimal neuronal layout problem. *Neural Comput* 16:2067–2078.
16. Salvador R, et al. (2005) Neurophysiological architecture of functional magnetic resonance images of human brain. *Cereb Cortex* 15:1332–1342.
17. Kaiser M, Hilgetag CC (2004) Spatial growth of real-world networks. *Phys Rev E Stat Nonlin Soft Matter Phys* 69:036103.
18. Kaiser M, Hilgetag CC (2004) Modelling the development of cortical networks. *Neurocomputing* 58:297–302.
19. Yook SH, Jeong H, Barabási A-L (2002) Modeling the Internet's large-scale topology. *Proc Natl Acad Sci USA* 99:13382–13386.
20. Latora V, Marchiori M (2001) Efficient behavior of small-world networks. *Phys Rev Lett* 87:198701.
21. Newman MEJ (2004) Fast algorithm for detecting community structure in networks. *Phys Rev E Stat Nonlin Soft Matter Phys* 69:066133.
22. Barabási A-L, Albert R (1999) Emergence of scaling in random networks. *Science* 286: 509–512.
23. Liu Y, et al. (2008) Disrupted small-world networks in schizophrenia. *Brain* 131: 945–961.
24. Lynall ME, et al. (2010) Functional connectivity and brain networks in schizophrenia. *J Neurosci* 30:9477–9487.
25. van den Heuvel MP, Mandl RCW, Stam CJ, Kahn RS, Hulshoff Pol HE (2010) Aberrant frontal and temporal complex network structure in schizophrenia: A graph theoretical analysis. *J Neurosci* 30:15915–15926.
26. Alexander-Bloch AF, et al. (2010) Disrupted modularity and local connectivity of brain functional networks in childhood-onset schizophrenia. *Front Syst Neurosci* 4:147.
27. Alexander-Bloch AF, et al. (2012) The anatomical distance of functional connections predicts brain network topology in health and schizophrenia. *Cereb Cortex*, 10.1093/cercor/bhr388.
28. Meunier D, Lambiotte R, Fornito A, Ersche KD, Bullmore ET (2009) Hierarchical modularity in human brain functional networks. *Front Neuroinform* 3:37.
29. van den Heuvel MP, Stam CJ, Kahn RS, Hulshoff Pol HE (2009) Efficiency of functional brain networks and intellectual performance. *J Neurosci* 29:7619–7624.
30. Li Y, et al. (2009) Brain anatomical network and intelligence. *PLOS Comput Biol* 5: e1000395.
31. Bassett DS, et al. (2009) Cognitive fitness of cost-efficient brain functional networks. *Proc Natl Acad Sci USA* 106:11747–11752.
32. Kitzbichler MG, Henson RNA, Smith ML, Nathan PJ, Bullmore ET (2011) Cognitive effort drives workspace configuration of human brain functional networks. *J Neurosci* 31:8259–8270.
33. Baars BJ (1988) *A Cognitive Theory of Consciousness* (Massachusetts Institute of Technology, Cambridge, MA).
34. Dehaene S, Naccache L (2001) Towards a cognitive neuroscience of consciousness: Basic evidence and a workspace framework. *Cognition* 79:1–37.
35. Kaiser M, Hilgetag CC (2006) Nonoptimal component placement, but short processing paths, due to long-distance projections in neural systems. *PLOS Comput Biol* 2:e95.
36. Cuntz H, Forstner F, Borst A, Häusser M (2010) One rule to grow them all: A general theory of neuronal branching and its practical application. *PLOS Comput Biol* 6: e1000877.
37. Fornito A, et al. (2011) Genetic influences on cost-efficient organization of human cortical functional networks. *J Neurosci* 31:3261–3270.
38. Perin R, Berger TK, Markram H (2011) A synaptic organizing principle for cortical neuronal groups. *Proc Natl Acad Sci USA* 108:5419–5424.
39. Rubinov M, et al. (2009) Small-world properties of nonlinear brain activity in schizophrenia. *Hum Brain Mapp* 30:403–416.
40. Bassett DS, et al. (2008) Hierarchical organization of human cortical networks in health and schizophrenia. *J Neurosci* 28:9239–9248.
41. Bullmore ET, Frangou S, Murray RM (1997) The dysplastic net hypothesis: an integration of developmental and dysconnectivity theories of schizophrenia. *Schizophr Res* 28:143–156.
42. Rapoport JL, Addington AM, Frangou S, Psych MRC (2005) The neurodevelopmental model of schizophrenia: Update 2005. *Mol Psychiatry* 10:434–449.
43. Fair DA, et al. (2009) Functional brain networks develop from a "local to distributed" organization. *PLOS Comput Biol* 5:e1000381.
44. Supekar K, Musen M, Menon V (2009) Development of large-scale functional brain networks in children. *PLoS Biol* 7:e1000157.
45. Honey CJ, Kötter R, Breakspear M, Sporns O (2007) Network structure of cerebral cortex shapes functional connectivity on multiple time scales. *Proc Natl Acad Sci USA* 104:10240–10245.
46. Doyle JC, et al. (2005) The "robust yet fragile" nature of the Internet. *Proc Natl Acad Sci USA* 102:14497–14502.
47. Cox RW (1996) AFNI: Software for analysis and visualization of functional magnetic resonance neuroimages. *Comput Biomed Res* 29:162–173.
48. Jenkinson M, Smith S (2001) A global optimisation method for robust affine registration of brain images. *Med Image Anal* 5:143–156.
49. Jenkinson M, Bannister P, Brady M, Smith S (2002) Improved optimization for the robust and accurate linear registration and motion correction of brain images. *Neuroimage* 17:825–841.
50. Burgund ED, et al. (2002) The feasibility of a common stereotactic space for children and adults in fMRI studies of development. *Neuroimage* 17:184–200.
51. Kang HC, Burgund ED, Lugar HM, Petersen SE, Schlaggar BL (2003) Comparison of functional activation foci in children and adults using a common stereotactic space. *Neuroimage* 19:16–28.
52. Fornito A, Zalesky A, Bullmore ET (2010) Network scaling effects in graph analytic studies of human resting-state FMRI data. *Front Syst Neurosci* 4:22.